inter.noise 2000
The 29th International Congress and Exhibition on Noise Control Engineering
27-30 August 2000, Nice, FRANCE

I-INCE Classification: 1.0

INNOVATIVE VIBROACOUSTIC CONTROL APPROACHES IN SPACE LAUNCH VEHICLES

S. Griffin*, S. Lane*, D. Leo**

* Air Force Research Laboratory, AFRL/VSDV, 3550 Aberdeen Ave SE, 87117, Kirtland Afb, United States Of America

** Virginia Polytechnic Institute and State University, Mechanical Engineering Department, 24061, Blacksburg, VA, United States Of America

Tel.: 1 505-846-9333 / Fax: 1 505-846-7877 / Email: griffins@plk.af.mil

Keywords:
ACTIVE, CONTROL, TRANSMISSION, LOW FREQUENCY

ABSTRACT
Vibroacoustics during space vehicle launch has been blamed for as many as 60% of first day satellite failures. At the Air Force Research Laboratory in Albuquerque NM USA, modeling and analysis was performed to determine the feasibility of various control approaches to reduce noise levels of the shroud interior. Candidate active actuation technologies included PMA's, piezoceramics and volume-velocity acoustic sources.

1 - INTRODUCTION

This paper combines the work of three feasibility studies on innovative active noise transmission reduction approaches directed at a specific launch vehicle [1,2]. Analytical studies using piezoceramics and proof mass actuators were accomplished using a modal interaction model along with an optimal control approach. The focus of these studies was to calculate the maximum performance of each approach when realistic constraints were imposed. The third study started with experimental results at relatively low acoustic levels. These results were then scaled to project the power and actuator requirements necessary to accomplish the same performance at more realistic acoustic levels. The objective in the first two studies was to reduce acoustic transmission directly, whereas the objective in the third study was to add dissipation to low frequency cavity modes. The goal of all three approaches is lower interior acoustic levels during launch.

2 - FEASIBILITY STUDIES

All three feasibility studies have in common the fairing geometry shown in Figure 1. The modal interaction model is given by

$$\begin{gathered}\dot{\mathbf{z}} = \begin{bmatrix} \mathbf{A} & \mathbf{B}''' \\ \mathbf{B}'' & \mathbf{A}' \end{bmatrix} \mathbf{z} + \begin{bmatrix} \mathbf{B} \\ \mathbf{0} \end{bmatrix} \mathbf{u} + \mathbf{H}\mathbf{v} \\ \mathbf{y} = \begin{bmatrix} \mathbf{C} & \mathbf{0} \end{bmatrix} \mathbf{z} \\ \mathbf{y}' = \begin{bmatrix} \mathbf{0} & \mathbf{C}'' \end{bmatrix} \mathbf{z}\end{gathered} \tag{1}$$

a fully coupled state space model specific to the fairing geometric and material properties [1]. In Equation 1, $\mathbf{z}$ includes both structural and acoustic states, $\mathbf{A}$, $\mathbf{B}$ and $\mathbf{C}$ result from the uncoupled structural model, $\mathbf{A}$' and $\mathbf{C}$" result from the uncoupled acoustic model, $\mathbf{B}$"' and $\mathbf{B}$" define structural acoustic coupling and $\mathbf{H}$ defines the acoustic disturbance path. The inputs to the state space model are external acoustic loading, $\mathbf{v}$, at each structural node and control inputs, $\mathbf{u}$. The outputs of the model are proportional to structural displacement as measured by piezoceramic and/or displacement sensors and internal acoustic pressure within the launch vehicle fairing.
The reverberant disturbance for the analytical studies was modeled as the blocked-surface pressure field [1] and applied to the fully coupled model as an external, time and spatial-varying pressure input.

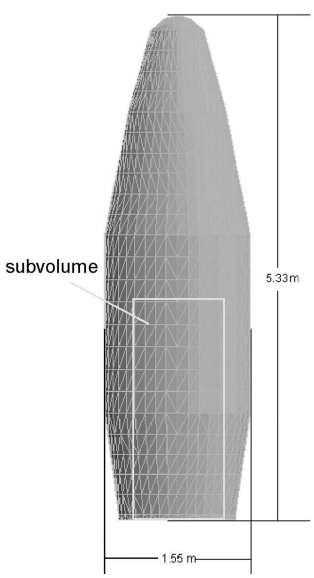

Figure 1: Geometry of launch vehicle fairing.

Optimal placement of sensors and actuators was determined based on a previous radiation mode approach to minimize the acoustic potential energy within a given subvolume of the launch vehicle fairing shown in Figure 1 [3]. The approach determines which structural mode shapes are most dominant in noise transmission. The constraint applied to both the analytical feasibility studies placed limitations on the number of actuators and the maximum power applied to each actuator. The weight of the actuators, control and power electronics was not to exceed 25% of the weight of the fairing. In this case, the fairing weight was modeled as 63.6 kg so the total added weight associated with each approach was limited to just under 16 kg.

2.1 - Feasibility study using piezoceramic actuators

In order to model the effect of integral piezoceramic actuators on the coupled structural/acoustic model, the structural part of the state space model given by Equation 1 was modified accordingly. The actuator model is developed from the coupled electromechanical equations of motion for piezoelectric materials. Mass and stiffness matrices are developed based on the derivation by Hagood, *et al*, for a general structure with piezoelectric elements [4]. The mass and stiffness matrices are derived using the shape functions for a Mindlin plate element [5]. The degrees of freedom are the transverse vibration and in-plane rotations at each of the four nodes of the element. The result is an element model of the standard second-order form

$$M^i_{pzt}\ddot{x}^i_{pzt} + Kx^i_{pzt} = F^i_{pzt}v^i_{pzt} \tag{2}$$

where the superscript i represents the equations of motion for the i^{th} actuator. The input to the actuator is the voltage v_{pzt}. Equation 2 represents the equations of motion for the piezoelectric material referred to local element coordinates. A coordinate transformation can be applied to transform Equation 2 into the coordinates of the fairing structural model. The modal equations for the fairing structure are augmented with the modal equations for each piezoelectric actuator

$$\left(I + \sum_i \Phi^T T^T M^i_{pzt} T_i \Phi\right)\ddot{r} + \left(\Lambda + \sum_i \Phi^T T_i^T K^i_{pzt} T_i \Phi\right) r = F_{ext} + \sum_i \Phi^T T_i^T F^i_{pzt} v^i_{pzt} \tag{3}$$

Equation 3 is then used to derive the **A** and **B** matrices of Equation 1. The actuator piezoceramics are also used as simultaneous sensors as suggested by Dosch [6] and Anderson and Hagood [7] with the sensed voltage of each simultaneous sensor/actuator related to the element degrees of freedom through the expression

$$y^i_{pzt} = kF^i_{pzt}x^i_{pzt} \tag{4}$$

where the output matrix is the transpose of the input matrix due to the reciprocity of strain and moment in the coupled electromechanical equations and the constant k is related to the capacitance of the

piezoceramic and signal conditioning used. It should be noted that the assumption of all of the actuator command voltage being applied to the actuator is not realizable in a simultaneous sensor/actuator implementation. It can, however, be realized approximately under certain signal conditioning implementations [6]. Equation 4 is used to derive the **C** matrix of Equation 1.

Having developed a model which predicts the effect of piezoceramics on the coupled structural acoustic model and having derived dominant structural mode shapes for sensor/actuator placement, the next step is to decide how many piezoceramics to incorporate into the model and where to locate them. For the piezoceramic feasibility study, two additional assumptions were made to aid in this task. It was assumed that of the 16 kg allowed, half would be piezoceramic weight- the other half being reserved for control and power electronics. Further, based on readily available piezoceramics, it was assumed that the thickness of the piezoceramics used would be.76 mm. With the weight and the thickness predetermined, the total actuator area was fixed at 1.36 m^2 by the density of the piezoceramic. The individual actuator locations were determined by evaluating the modal coupling to the dominant structural mode shapes for each possible actuator location on the fairing. In this case, the number of actuator locations is determined by the number of unconstrained structural elements. These modal coupling results were rank ordered and the weight of the piezoceramics covering the top 20 locations corresponded to just under 8 kg.

With the actuator positions established, it was possible to use LQG optimal control to formulate a controller to reduce noise transmission into the fairing. An output weighting was selected to directly penalize noise transmission. The control effort penalty was decreased until the feedback voltage applied to the piezoceramic corresponded to the maximum recommended. This was judged to be the limiting performance of the approach. The resulting RMS reduction within these constraints was only 1.25 dB. As a check on the approach, the open-loop disturbance level was reduced to that the internal level was 120 dB RMS. For this reduced level, the maximum achievable reduction was an only slightly better 1.65 dB RMS.

2.2 - Feasibility study using proof-mass actuators

Proof mass actuators were also evaluated as actuators in an optimal control approach. In this case, the entire weight margin was allotted for the proof mass actuators, and no allowance was made for control and power electronics. By making this assumption, the best achievable results were sought, and, if promising, a more realistic division of weights was to be evaluated. The actuator parameters were based on an off-the-shelf proof-mass actuator, the Aura AST-2B-04. It was assumed that the weight of the housing and the heat sink could be reduced slightly due to the relatively short duration of required performance during the initial stage of launch. It was also assumed that the maximum RMS power limit of 75 Watts could be relaxed to 100 Watts over the relatively short performance lifetime. An increased actuator constant of twice the actual constant, ψ, was assumed to allow for improved actuator performance, and likewise the coil resistance and inductance were also doubled. The resulting actuator weight was 1.3 kg, allowing 12 actuators for control.

Similar to the piezoceramic study, the locations for the actuators were selected as the top 12 nodal locations to couple into the important structural mode shapes. The augmented structural state space model was calculated based on a simple spring mass / electromagnetic model for a voice coil given in reference 1. This gave the structural **B** matrix of Equation 1. Since the addition of the PMA's had a significant effect on the structural behavior of the fairing, it was necessary to model the PMA's in the FEM code to get new structural frequencies and mode shapes required in the modal interaction model. Collocated displacement sensors were assumed to be an integral part of the PMA assemblies, and this assumption gave the structural **C** matrix in Equation 1.

As in the piezoceramic study, acoustic transmission was penalized directly in the optimal control problem and the control effort penalty was decreased to the point where the 100 watt limit was reached on the PMA's. The resulting RMS reduction was a respectable 4.2 dB RMS reduction. However, a simulation of noise reduction with the loop open yielded 3.5 dB RMS reduction. The inescapable conclusion was that the majority of the reduction in noise transmission that results due to the introduction of PMA's was due to their passive effects and the additional performance achieved by closing the loop with the power constrained was relatively small. The passive effect of the PMA's can be attributed to two predominant mechanisms. First, there was the addition of structural damping to the fairing modes by the heavily damped PMA's. Damping in PMA's is attributable to both structural damping and the back-EMF, which is proportional to the out-of-plane velocity. Second, the introduction of a spring-mass-damper at a point of large out-of-plane displacement in the dominant structural modes reduced the effectiveness of those modes in transmitting the acoustic disturbance to the fairing interior. A final closed-loop simulation was done with the allowable power to the PMA's increased to 200 watts. The resulting reduction under this new constraint was still only 4.5 dB RMS.

2.3 - Scaled experiment feasibility study

The final study was based on extrapolation of experimental results for a novel active acoustic control approach to reduce the low frequency acoustic modal response of a fairing. The control method uses spatially weighted transducer arrays with H_2 feedback control laws to globally attenuate the low frequency acoustic modes in the fairing. Loudspeakers were compensated to approximate constant volume-velocity sources [8] and were used as control actuators, while microphones were used as pressure sensors. The sensors and actuators were collocated and spatially weighted to sense or couple to target modes. Sensor and actuator weights were related to the mode shape of the structure and the relative positions of the sensors and actuators [9].

An additional loudspeaker was placed in the fairing and used to create a disturbance for measuring the closed-loop reduction. In addition to the sensor microphones, performance microphones were placed in the fairing at arbitrary positions to measure the pressure response away from the actuators. Controller performance was measured averaging the open-loop and closed-loop frequency responses from the disturbance to the sensor microphones and the performance microphones. By considering the averaged response measured at the sensor microphones, the effect of the controller on the sound field close to the control actuators can be determined. Likewise, by considering the averaged response measured by the performance microphones, the effect of the controller on the overall interior acoustic response can be observed. These responses indicate the amount of reduction of the targeted acoustic modes, and also show spillover if any occurs.

In addition to controller performance, issues such as actuator power requirements and actuator diaphragm displacement were considered in this investigation. Although relatively low sound pressure levels were generated in these experiments (approximately 89 dB), the RMS power and diaphragm displacement can be extrapolated to higher sound pressure levels using the transfer functions from the sensors to the actuators. The power consumed by the actuators for a given interior disturbance level measured by the sensor microphones can be estimated based on frequency response measurements. Also, by knowing the displacement response of the actuators for a given control input level, the diaphragm excursions can also be predicted for a given disturbance level.

A correct scale fiberglass model of the fairing shown in Figure 1 was constructed and used as a testbed. Experiments were conducted using sixteen constant volume-velocity actuators with sixteen collocated sensor microphones and sixteen performance microphones. The actuators used in this experiment were off-the-shelf 14-cm loudspeakers rated to have 100 Watt power handling capability. The fairing model was approximately 5.3 meters in length, 1.3 meters in diameter (maximum), and tapered at both ends. An aluminum end cap was fixed to the nose, and a plywood end cap was attached to the base. Each sensor and actuator pair was rigidly attached to the composite structure. The sensor and actuator pairs were evenly distributed along the length and circumference of the fairing interior to yield even spatial sampling. All cabling was connected through a panel at the base of the fairing. The controller, spectrum analyzers, power amplifiers, microphone conditioners, and other required hardware were stored on the outside of the fairing.

The results from a controller designed to attenuate the first three low frequency modes of the fairing are presented in Figure 2. The first and second modes were reduced by approximately 10 dB, and the third by 5 dB, both at the sensor microphones and the performance microphones. The controller had little affect on the non-target modes, which is desirable from a stability standpoint. Over the 200 Hz bandwidth, the controller yielded an overall reduction in the RMS response at the sensor microphones of 3.46 dB, and of 3.30 dB at the performance microphones. Using this controller, the power requirements and actuator diaphragm displacement were computed and extrapolated to higher disturbance levels. Results of these calculations showed that the diaphragm displacement was less than two millimeters for disturbance levels up to 120 dB. This displacement is well within the linear excursion range of typical actuators. However, for disturbance levels of 140 dB, the predicted excursion was on the order of several millimeters, which would require modification or redesigning of the actuator. Likewise, the power delivered to the actuators was within the allowable range up to disturbance levels of 120 dB. Above 120 dB, actuators began exceeded the 100 Watt rating. At 130 dB, there were several actuators above the nominal rating, and at 140 dB, the simulation indicated power levels in the kilowatt range. The data indicates that the power requirements increase two orders of magnitude for every 20 dB increase in the disturbance level.

3 - CONCLUSIONS

While all of the approaches investigated exhibited shortcomings in the presence of realistic constraints, further research is indicated in several areas. An investigation of the passive reduction due to introduction of the PMA's is underway to evaluate the feasibility of a passive device combining a change of both

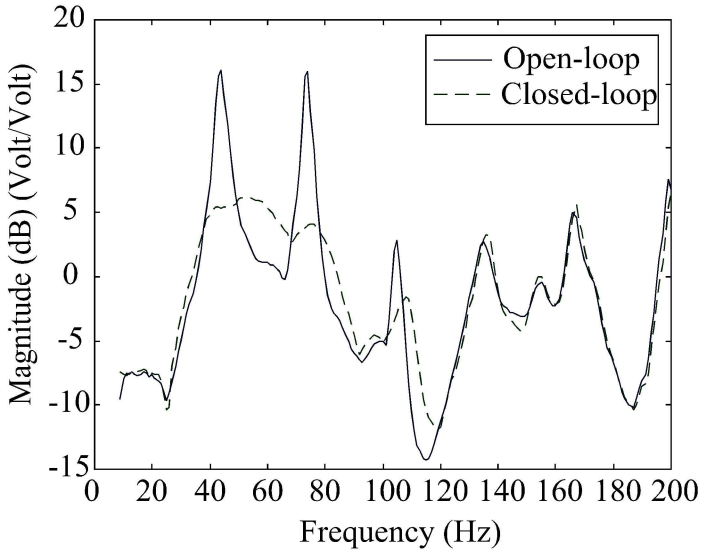

Figure 2: Average performance microphone response for the three-mode controller.

structural and acoustic impedance geared at reducing low frequency transmission. Further investigation of the volume-velocity approach is also underway with the goal of a hybrid combination of this and the passive approach.

REFERENCES

1. **Griffin, S., Hansen, C. and Cazzolato, B.**, Feasibility of feedback control of transmitted sound into a launch vehicle fairing using structural sensing and proof mass actuators, In *AIAA/ASME/ ASCE/AHS/ASC Structures, Structural Dynamics, and Materials Conference*, pp. 2592-2602, 1999

2. **Lane, S., Kemp, J., Clark, R. and Griffin, S.**, Feasibility Analysis for Active Acoustic Control of a Rocket Fairing using Spatially Weighted Transducer Arrays, In *AIAA/ASME/ASCE/AHS/ ASC Structures, Structural Dynamics, and Materials Conference*, 2000

3. **Griffin, S., Hansen, C., Cazzolato, B**, Feedback Control of Structurally Radiated Sound into Enclosed Spaces using Structural Sensing, *J. Acoust. Soc Am.*, Vol. 106(5), pp. 2621-2628, 1999

4. **Hagood, N., Chung, W., von Flotow, A.**, Modeling of Piezoelectric Actuator Dynamics for Active Structural Control, *Journal of Intelligent Material Systems and Structures*, Vol. 1 (3), pp. 327-354, 1990

5. **Cook, R.D., Malkus, D.S., Plesha, M.E.**, *Concepts and Elements of Finite Element Analysis, 3rd Edition*, John Wiley and Sons, New York, NY, 1989

6. **Dosch, J., Inman, D. and Garcia, E.**, A self-sensing piezoelectric actuator for collocated control, *Journal of Intelligent Material Systems and Structures*, Vol. 3, pp. 166-185, 1992

7. **Anderson, E. and Hagood N.**, Simultaneous Piezoelectric Sensing/Actuation: Analysis and Application to Controlled Structures, *J. of Sound and Vib.*, Vol. 174(5), pp. 617-639, 1994

8. **Lane, S. and Clark, R.**, Improving Loudspeaker Performance for Active Noise Control Applications, *Journal of the Audio Engineering Society*, Vol. 46(6), pp. 508-519, 1998

9. **Lane, S., Clark, R., and Southward, S.**, Active Control of Low Frequency Modes in an Aircraft Fuselage Using Spatially Weighted Arrays, *accepted for publication in the Journal of Vibration and Acoustics*